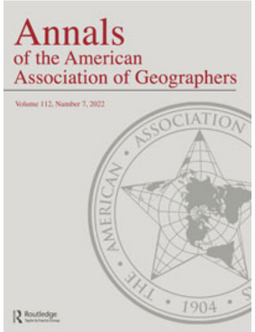

Taylor & Francis
Taylor & Francis Group

Annals of the American Association of Geographers

ISSN: (Print) (Online) Journal homepage: https://www.tandfonline.com/loi/raag21

Measuring Physical Disorder in Urban Street Spaces: A Large-Scale Analysis Using Street View Images and Deep Learning

Jingjia Chen, Long Chen, Yan Li, Wenjia Zhang & Ying Long

To cite this article: Jingjia Chen, Long Chen, Yan Li, Wenjia Zhang & Ying Long (2022): Measuring Physical Disorder in Urban Street Spaces: A Large-Scale Analysis Using Street View Images and Deep Learning, Annals of the American Association of Geographers, DOI: 10.1080/24694452.2022.2114417

To link to this article: https://doi.org/10.1080/24694452.2022.2114417

View supplementary material

Published online: 14 Oct 2022.

Submit your article to this journal

View related articles

View Crossmark data

Full Terms & Conditions of access and use can be found at
https://www.tandfonline.com/action/journalInformation?journalCode=raag21

Check for updates

Measuring Physical Disorder in Urban Street Spaces: A Large-Scale Analysis Using Street View Images and Deep Learning

Jingjia Chen,[*] Long Chen,[†] Yan Li,[*] Wenjia Zhang,[‡] and Ying Long[§]

[*]*School of Architecture, Tsinghua University, China*
[†]*Beijing Key Laboratory of Traffic Engineering, Beijing University of Technology, China, and School of Architecture, Tsinghua University, China*
[‡]*Peking University Shenzhen Graduate School, China*
[§]*School of Architecture and Hang Lung Center for Real Estate, Key Laboratory of Eco Planning & Green Building, Ministry of Education, Tsinghua University, China*

Physical disorder is associated with negative outcomes in economic performance, public health, and social stability, such as the depreciation of property, mental stress, fear, and crime. A limited but growing body of literature considers physical disorder in urban space, especially the topic of identifying physical disorder at a fine scale. There is currently no effective and replicable way of measuring physical disorder at a fine scale for a large area with low cost, however. To fill the gap, this article proposes an approach that takes advantage of the massive volume of street view images as input data for virtual audits and uses a deep learning model to quantitatively measure the physical disorder of urban street spaces. The results of implementing this approach with more than 700,000 streets in Chinese cities—which, to our knowledge, is the first attempt globally to quantify the physical disorder in such large urban areas—validate the effectiveness and efficiency of the approach. Through this large-scale empirical analysis in China, this article makes several theoretical contributions. First, we expand the factors of physical disorder, which were previously neglected in U.S. studies. Second, we find that urban physical disorder presents three typical spatial distributions—scattered, diffused, and linear concentrated patterns—which provide references for revealing the development trends of physical disorder and making spatial interventions. Finally, our regression analysis between physical disorder and street characteristics identified the factors that could affect physical disorder and thus enriched the theoretical underpinnings. *Key Words: deep learning, physical disorder, street view image, urban street space.*

Physical disorder, or neighborhood physical disorder in urban space, refers to the disturbance in residents' lives and public spaces caused by observable or perceptible visual signs (Skogan 1990). Evidence indicates that physical disorder is an external representation of urban decay and is associated with crimes, such as theft, robbery, and prostitution (Skogan 1990; Ross and Jang 2000). Additionally, the epidemiology community has found that residents who live in environments with higher levels of physical disorder tend to suffer from greater stress and fear, which could trigger unhealthy behaviors (e.g., binge drinking; Keyes et al. 2012) and adverse outcomes (e.g., obesity; Burdette and Hill 2008). Therefore, the physical disorder of urban space has become an interdisciplinary subject at the nexus of urban planning, social science, and public health, attracting attention from both academics and practitioners.

With the expansion of our knowledge of urban streets, the function of streets has been redefined from mobility to livability, and streets have become important components of urban space that support various human activities. Given that urban streets as public spaces exert significant impacts on quality of life, the spatial quality of urban streets has become of great interest. Quantifying the quality of urban space, such as physical disorder, remains a central issue for both researchers and planners, however. Conventional measurements of physical disorder rely heavily on systematic social observations (SSOs) or neighborhood audits (Sampson and Raudenbush 1999), which are expensive, time-consuming, and sometimes dangerous (Grubesic et al. 2018); thus, they are usually limited in both geographic and temporal coverage. In addition, potential bias exists when different auditors observe the same space, as

Annals of the American Association of Geographers, 0(0) 2022, pp. 1–19 © 2022 by American Association of Geographers
Initial submission, February 2021; revised submissions, December 2021, April and July 2022; final acceptance, July 2022
Published by Taylor & Francis, LLC.

they assess the environment based on what they visually observe, which might not reflect the objective physical environment. Due to the rapid development of online mapping services, street view images (SVIs) that record the urban landscape along streets have become publicly accessible, providing an alternative approach for auditing physical disorder. As a new type of data source, the SVIs not only break through spatial-temporal limitations, but also provide abundant information on urban street landscapes (F. Zhang et al. 2018) and have been used in virtual auditing studies (e.g., Mooney et al. 2016; Jiang et al. 2018). Although evidence is accumulating that virtual auditing with SVIs is an effective alternative in quantifying and understanding our built environment, the studies that use such data and methods in physical disorder identification remain limited. In addition, existing studies that use SVIs for virtual auditing still require extensive manual auditing of each image, which can now be performed much more efficiently by computer vision and image processing. In addition, the existing literature on assessing physical disorder is either based on Western cities or a limited number of sample areas, which also encourages us to initiate a large-scale analysis in the Chinese context.

In the past decade, the advancement of deep learning models has resulted in great progress in image processing. Due to its ability to automatically learn image features and accurately recognize various objects, deep learning could supersede conventional manual audits and provide an opportunity for the large-scale, automatic measurement of physical disorder using SVI data. Aiming to fill the potential gaps in quantifying physical disorder, this article proposes an approach that combines SVIs and deep learning to automatically measure the physical disorder of urban streets, which can manifest as abandoned buildings, vacant lots covered by ruderal and trash, and so on, in the SVIs. The results of implementing this methodology on more than 700,000 streets in 264 cities in China—to the best of our knowledge, the first attempt to use large amounts of SVI data and deep learning algorithms in quantifying large-scale, street-level physical disorder for a number of cities—validate the effectiveness and efficiency of the method. In addition to the great methodological innovation, there are several theoretical contributions through the large-scale empirical study in China. First, we enriched the indicator system of physical disorder, which has been mostly ignored in previous studies in a U.S. context. Second, we find that urban physical disorder exhibits three spatial characteristics: monocentric, sectoral, and polycentric patterns. Further, the probability of disorder in street space is positively associated with street length, functional combination, and distance to urban centers, but negatively correlated with the functional density of streets and the density of intersections, which provides opportunities for locating disordered streets, assessing development trends, and making spatial interventions.

Literature Review

Measuring Physical Disorder with Conventional Methods

Physical disorder is recognized as the presence of specific visual items on the street and exerts a negative impact on individuals' perceptions of the comfort and safety of the space (Franzini et al. 2008). For example, in the Project on Human Development in Chicago Neighborhoods, approximately 90 percent of the respondents believed that garbage or broken glass on the street or sidewalks indicated disorder (Sampson and Raudenbush 1999). The presence of window bars on buildings made nearly half of the people in one survey more likely to judge the space as being disordered (Day et al. 2006). Therefore, to achieve a full understanding of the impacts of physical disorder and its mechanisms, it is necessary to conduct a large-scale and comprehensive measurement of these disorder-related visual items.

Traditional methods of measuring physical disorder include telephone interviews, field questionnaires, and SSOs, all of which are both labor- and cost-intensive processes. Moreover, auditors sometimes have to take risks to enter potentially dangerous areas, as physical disorder has been found to be associated with crime (Taylor, Shumaker, and Gottfredson 1985; Perkins, Meeks, and Taylor 1992). Sampson and Raudenbush (1999) carried out an SSO with the aid of video-recording technology, which partially solved the problem of in-person auditing. Such a method, however, can neither be applied to large-scale measurements nor deliver comparable results across time and space (Jones, Pebley, and Sastry 2011).

Due to the availability of massive SVI data and the development of omnidirectional image technology with high resolution, virtual auditing through SVIs has become an effective alternative to environmental auditing due to its wider spatial coverage, higher SVI update frequency, and lower acquisition cost. Physical disorder studies have also switched to virtual auditing methods using SVIs (e.g., Clarke et al. 2010; Mooney et al. 2014; Bader et al. 2015; Quinn et al. 2016; Mayne, Pellissier, and Kershaw 2019). For example, Quinn et al. (2016) visualized the distribution of physical disorder in New York City through virtual audits and found that wide swaths of disorder were concentrated in most of the Bronx and the northernmost part of the borough, away from the city center. Other than SVIs from online map platforms, scholars also tried to collect primary SVIs at the human scale. Using wearable cameras and virtual audits, Z. Zhang et al. (2021) and Li et al. (2022) assessed small-scale, individual exposure to urban greenery and neighborhood physical disorder, respectively. Such studies using SVIs and virtual audits, however, depend on manual audits of the images, and limitations in terms of geographic and temporal constraints remain significant.

Auditing Street View Images with Deep Learning Models

The development of high-performance computing systems and the availability of large-scale annotated data sets offers a new opportunity for the large-scale, automated processing of SVIs using deep learning algorithms (F. Zhang et al. 2018). Convolutional neural networks, as classic deep neural networks, can be trained for feature extraction of an SVI and then effectively identify elements in the street space, including but not limited to sidewalks, vehicles, buildings, and green plants (Shen et al. 2018; Tang and Long 2019). One such network, Cambridge University's SegNet, uses a method that enables a deep learning framework to conduct semantic segmentation of SVIs, resulting in high-quality segmentation (Kendall, Badrinarayanan, and Cipolla 2015). In addition, Suel et al. (2019) applied deep learning and street view imagery to reveal through an audit of SVIs that London's highest income areas are located in the city center and the southwest, where the scores of spatial quality are the highest. Due to the availability of the massive volume of SVI data and the advances in deep learning algorithms, using deep learning to extract considerable potential information from SVIs has also been employed in the evaluation of street greenery (Helbich et al. 2019; Ye et al. 2019; Z. Zhang et al. 2021), public health (Keralis et al. 2020; Nguyen et al. 2020), and street safety (Naik et al. 2014), all of which laid methodological foundations for our study on physical disorder assessment using SVI and deep learning. The lack of large-scale analysis on physical disorder is an additional reason we carried out this study.

Method

Study Area

For Chinese cities, the administrative boundary is much larger than their spatial region, leading the cities to include both urban areas and rural areas. Thus, this research adopted Ma and Long's (2020) spatial city data, which use communities as basic administrative units and the data of urban built-up areas to identify urbanized areas. Superimposing the available street view imagery over the spatial city boundary, we finally used the data set of 264 prefecture-level or above cities[1] in China (see Figure 1), which includes 769,407 streets in total and covers most urban areas of China with the latest SVIs.

Data

The SVIs in 264 Chinese cities are the core data set in this study. We used the 2014 roads and streets of China obtained from Amap (https://mobile.amap.com/), a local road-navigation firm based in Beijing, for crawling SVIs. We clipped the data set with the study area and derived the street segments within the study area and also removed highways and bridges to avoid the street-level images captured in them, resulting in 769,407 streets with a total length of 155,063 km. Then the Tencent Maps application programming interface (API) was used to query and download SVIs (see https://lbs.qq.com/panostatic_v1/guide-getImage.html, accessed June 27, 2022). The sampling points on the streets were first generated on the map at an interval of 100 m (50 m in Beijing). Each point has latitude, longitude, and other parameters to facilitate the crawling processes. Furthermore, by concatenating the parameters, including size (1,280 * 720), pitch (0), heading (0,

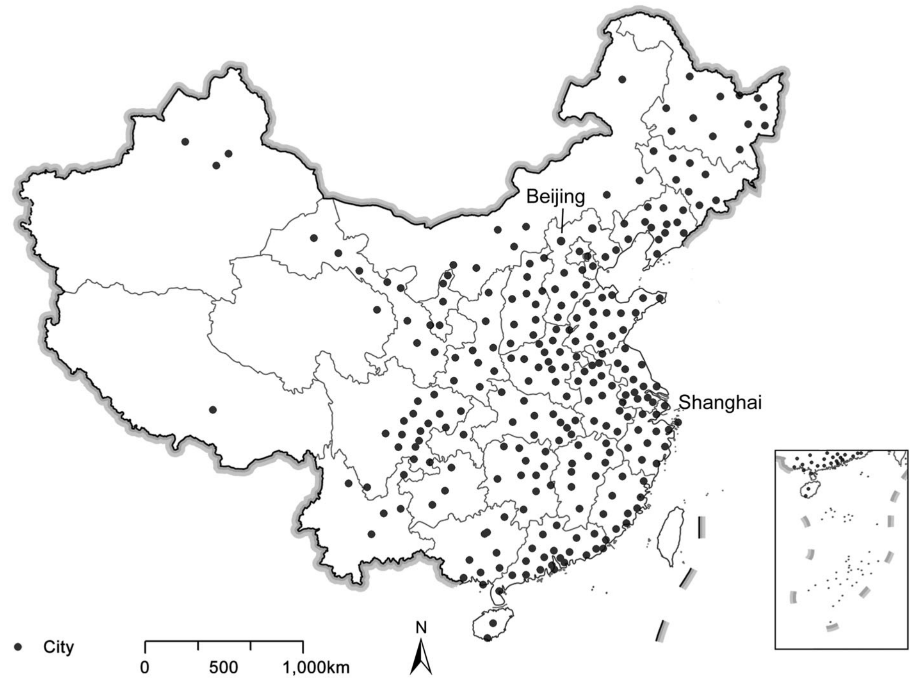

Figure 1. Location of 264 cities in China.

90, 180, and 270 for four directional SVIs), and the request key, we could obtain a URL to open the street view Web site pages. Afterward, with the support of Python, we downloaded the SVIs in four directions—north, west, east, and south—for each sampling point. Finally, a total of 4,876,952 SVIs in 2015 were collected, representing 1,219,238 sampling points on all the streets within 264 Chinese cities.

Defining and Identifying Physical Disorder in Chinese Cities

The first step is to create an indicator system of physical disorder for Chinese cities. First, in accordance with the previous studies (Sampson and Raudenbush 1999; Day et al. 2006; Quinn et al. 2016), a checklist containing a comprehensive set of physical disorder factors was constructed. Second, seven auditors with professional backgrounds either in architecture or urban planning conducted a few field surveys in random streets in Beijing, and also performed a virtual audit with 1,000 randomly selected SVIs (from all 4,876,952 SVIs in 264 cites) to compare what they found with the indicators in the checklist. Factors that were not found in both the SVIs and the field surveys, such as empty bottles and cigarette butts, were removed from the checklist, and some new factors that are commonly seen in the sample SVIs or field surveys, which are also manifestations of the physical disorder according to the definition, such as illegal or temporary buildings, street vendors, and unpaved roads, were added to the list. Finally, a refined list with five categories and fifteen detailed factors was created to represent the physical disorder indicators in urban streets (see Figure 2). For each factor, a sample image is provided to demonstrate how the factor manifested and can be identified in the SVIs.

Virtual Auditing of the Training Set

The second step is to generate a training set for the deep learning model. To minimize the statistical error and potential bias caused by cognitive differences between auditors, auditors were trained to do experimental audits on 5,000 sample images (randomly selected from the 4,876,952 SVIs in 264 Chinese cities) after receiving formal research and training materials, and interrater reliability (IRR) was calculated using the Kappa index (Vanwolleghem et al. 2016) until it was above 80 percent (Landis and Koch 1977) before proceeding to the formal scoring, which was performed with 200,000 randomly selected SVIs from all the SVIs to identify the physical disorder. Based on a predefined auditing guideline for each physical disorder factor, the auditors provided a general judgment

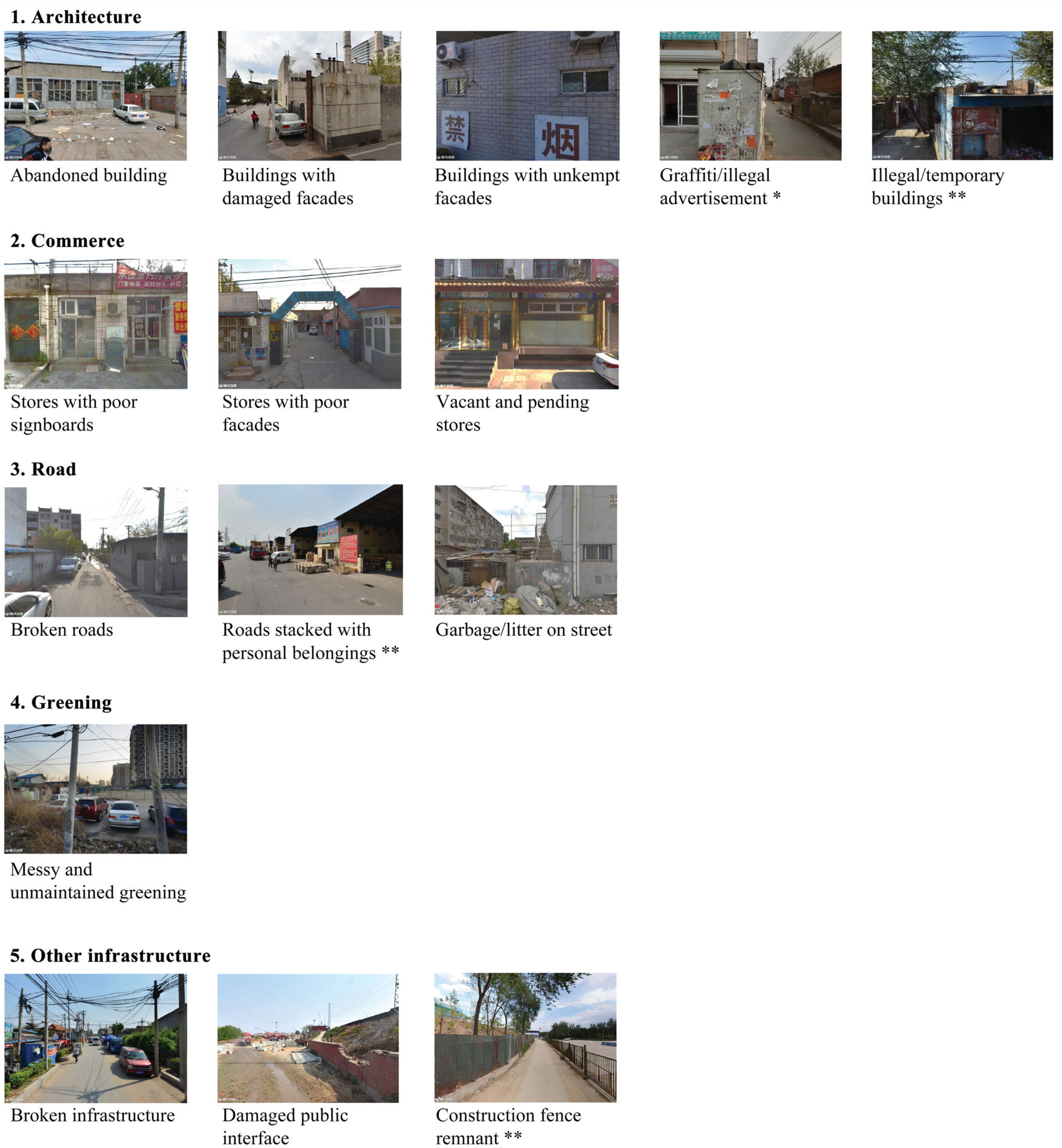

* Factors that are manifested largely differently from previous studies.
** New factors that reflect the unique urban landscape in Chinese cities.
Data source: Tencent Street View images in 2015

Figure 2. Reference samples of physical disorder factors.

on whether any factor of physical disorder existed in each SVI. If one physical disorder factor was identified, the image was assigned a score of 1; otherwise, it was given a score of 0. Only images labeled 1 for 15 categories of physical disorder were selected for training. In Table 1, the second column lists the number

Table 1. Performance of each model for physical disorder factors

Physical disorder factors	Number of training images	Percentage (%)	Accuracy (%)	Cross-entropy
Abandoned buildings	598	0.6	84.1	91.8
Buildings with damaged facades	4,210	4.2	53.4	62.3
Buildings with unkempt facades	15,902	15.9	79.9	88.3
Graffiti/illegal advertisement	12,645	12.6	80.7	72.6
Illegal/temporary buildings	4,618	4.6	51.6	58.6
Stores with poor signboards	6,427	6.4	74.6	78.4
Stores with poor facades	2,843	2.8	59.8	59.9
Vacant and pending stores	2,736	2.7	60.3	67.6
Messy and unmaintained greening	7,726	7.7	81.8	81.7
Garbage/litter on street	5,096	5.1	82.4	84.3
Construction fence remnant	626	0.6	69.9	69.7
Broken roads	13,061	13.1	80.5	83.6
Roads stacked with personal belongings	1,074	1.1	67.6	68.6
Broken infrastructure	11,224	11.2	81.0	78.6
Damaged public interface	2,964	3	84.1	72.1

Table 2. MobileNet V3-small structure

Type / Stride	Operator	exp Size	#out
224*224*3	Conv2d, 3*3	—	16
112*112*32	bneck, 3*3	16	16
56*56*16	bneck, 3*3	72	24
28*28*24	bneck, 3*3	88	24
28*28*24	bneck, 5*5	96	40
14*14*40	bneck, 5*5	240	40
14*14*40	bneck, 5*5	240	40
14*14*40	bneck, 5*5	120	48
14*14*48	bneck, 5*5	144	48
14*14*48	bneck, 5*5	288	96
7*7*96	bneck, 5*5	576	96
7*7*96	bneck, 5*5	576	96
7*7*96	conv2d, 1*1	—	576
7*7*576	pool, 7*7	—	—
1*1*576	conv2d 1*1, NBN	—	1,280
1*1*1280	conv2d 1*1, NBN	—	15

of training images for each category. All images labeled 1 are included in the training. The distribution of each category is shown as a percentage, which means the number of images labeled 1 out of a total number of 200,000 labeled images (see Table 1).

Identifying Physical Disorder Using a Deep Learning Model

Because this study deals with a huge amount of data, a lightweight and efficient machine learning algorithm is needed to make fast predictions. MobileNet is our first choice due to the advantages of fewer parameters, less computation, and shorter inference time. The structure of MobileNet V3-small is listed in Table 2 (Howard et al. 2019). In the model, the width multiplier, input resolution, batch size, and learning rate are set to 1, 224, 16, and 0.0001, respectively. Using the trained model, we obtain a classification result for each image, indicating the probability of the existence of a certain physical disorder factor.

Identifying Multiscale Spatial Patterns of Physical Disorder

The deep learning results of physical disorder are aggregated at three levels: sampling points, streets, and cities. Specifically, the physical disorder probability of each sampling point is the arithmetic average of disorder probability of four-directional SVIs (see Equation 1; the overall disorder probability of each image is the arithmetic average of the disorder probability of fifteen factors). The disorder probability of one street is the arithmetic average of the disorder probability of sampling points contained in the street (Equation 2). The disorder probability of one city is the arithmetic average of the disorder probability of sampling points contained within the central urban area of the city (Equation 3).

$$D = \frac{\sum_1^4 p_j}{4} \tag{1}$$

$$D_{street\_k} = \frac{\sum_1^n D_{point\_i}}{n} (i = 1, \ldots, n) \tag{2}$$

$$D_{city\_l} = \frac{\sum_{1}^{m} D_{point\_i}}{m} (i = 1, \ldots, m) \tag{3}$$

where D_{point_i} is the disorder probability of sampling point i; p_j is the disorder probability of the SVI in direction j, $j = 1, 2, 3, 4$, referring to the north, south, west, and east directions, respectively; D_{street_k} is the disorder probability of street k; n is the number of sampling points in street k; D_{city_l} is the disorder probability of city l; and m is the number of sampling points in city l.

We use the tenfold cross-validation method by randomly dividing the data set into ten mutually exclusive subsets of similar size, using 90 percent as the training set each time and the remaining 10percent as the testing set. During the training, cross-entropy is used for classification, and after training, the accuracy rate is used for validation and testing. The accuracy is calculated by dividing the number of correct items by the number of all items. Cross-entropy is formulated as follows, where C represents the number of factors, p_i refers to the ground truth, and q_i refers to the prediction.

$$CE = \sum_{i=1}^{C} p_i \log(q_i) \tag{4}$$

After knowing the predicted results of physical disorder in Chinese cities, we further explored the distribution and genetic mechanism of physical disorder. Regression analysis is also conducted using the level of physical disorder as the dependent variable and some selected street attributes as the independent variables. The regression analysis reveals the associations between physical disorder in urban street spaces and street length, function density, function mix, junction density, and distance to the city center, which further helps us to find clues regarding how physical disorder appeared and how to renovate the street space, which is expressed by Equation 5:

$$Y_i = \beta_0 + \sum \beta_i X_i + \varepsilon \tag{5}$$

where Yi is the dependent variable, the disorder probability of street i; Xi is the influencing factor; β_0 is the constant and β_i is the coefficient (weight) of the corresponding influencing factor; and ε is the random error term.

In addition, spatial analysis tools in ArcGIS, such as the spatial join, hot spot analysis, and natural breaks methods, are also used to conduct the data analysis and then identify the patterns of disordered street space in Chinese cities.

Results

Performance of the Deep Learning Algorithm

Table 1 shows the performance of the MobileNet V3 model for each factor on the sample data set, with an average accuracy of 72.77 percent for the overall task. The accuracy for abandoned buildings and damaged public interface was slightly higher, at 84.1 percent. The accuracy of illegal or temporary buildings and buildings with damaged structure in the model was relatively low, at below 60 percent. The model performance can be further enhanced, however, by collecting more labeled data.

Identifying Features of Physical Disorder at the Street Level

The results (the data set supporting the conclusions is available in the Acknowledgment) of the deep learning show that physical disorder is quite common in Chinese cities, with more than half of the streets (74.2 percent) having at least one physical disorder factor (score > 0), but with a low overall disorder value of 0.213 on average, implying the presence of about three disorder factors. Furthermore, the probability distribution of street factors follows an exponential distribution, with most streets either having no factors or a low probability of physical disorder. In contrast, a few streets have a high probability of physical disorder factors (see Figure 3). Two typical images that represent a mean and high level of probability are illustrated in Figure 4.

Figure 5 offers a closer look at the deep learning results and compares the factor rankings with the preceding similar studies. As shown in Figure 5, one significant distinction is that some factors that were crucial in the preceding studies, which were mostly focused on U.S. cities, are relatively trivial in our study (e.g., housing vacancies and abandoned buildings). In contrast, the newly added factors that reflect the unique urban landscape with poor space quality had a higher probability (e.g., buildings with damaged facade and broken roads). For all fifteen

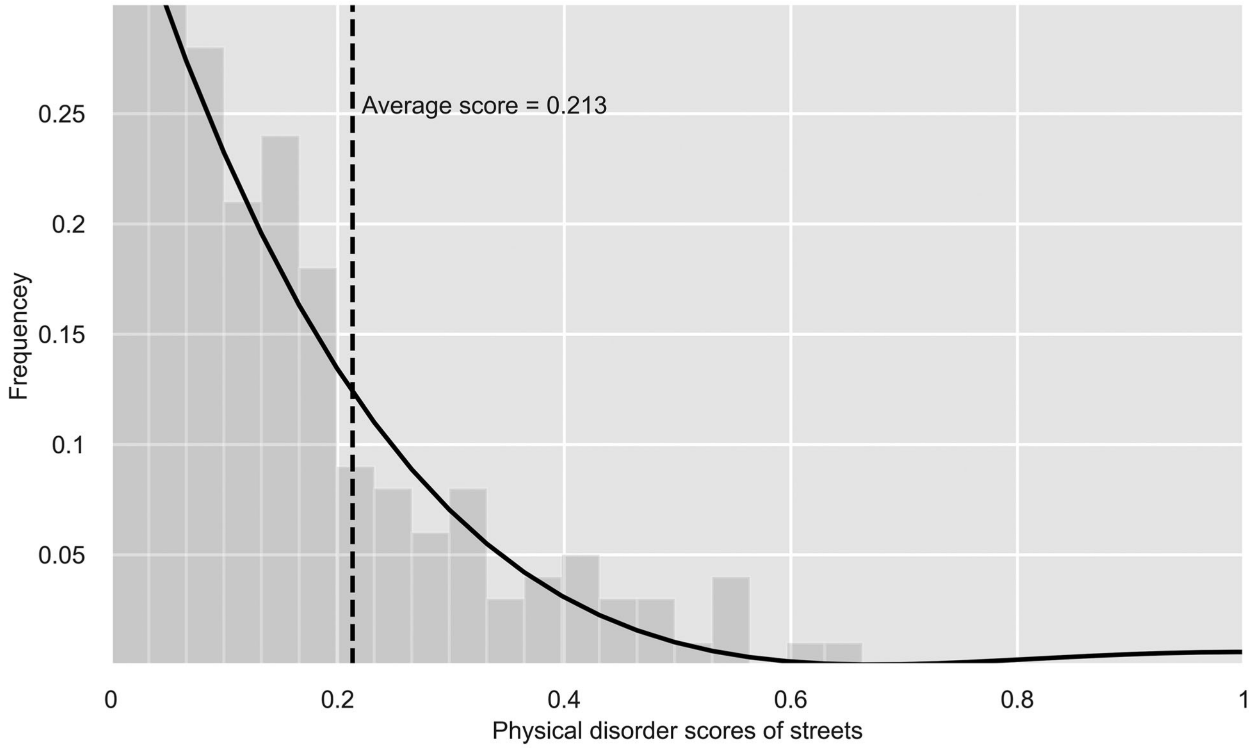

Figure 3. Distribution of the probability of physical disorder and the corresponding number of streets.

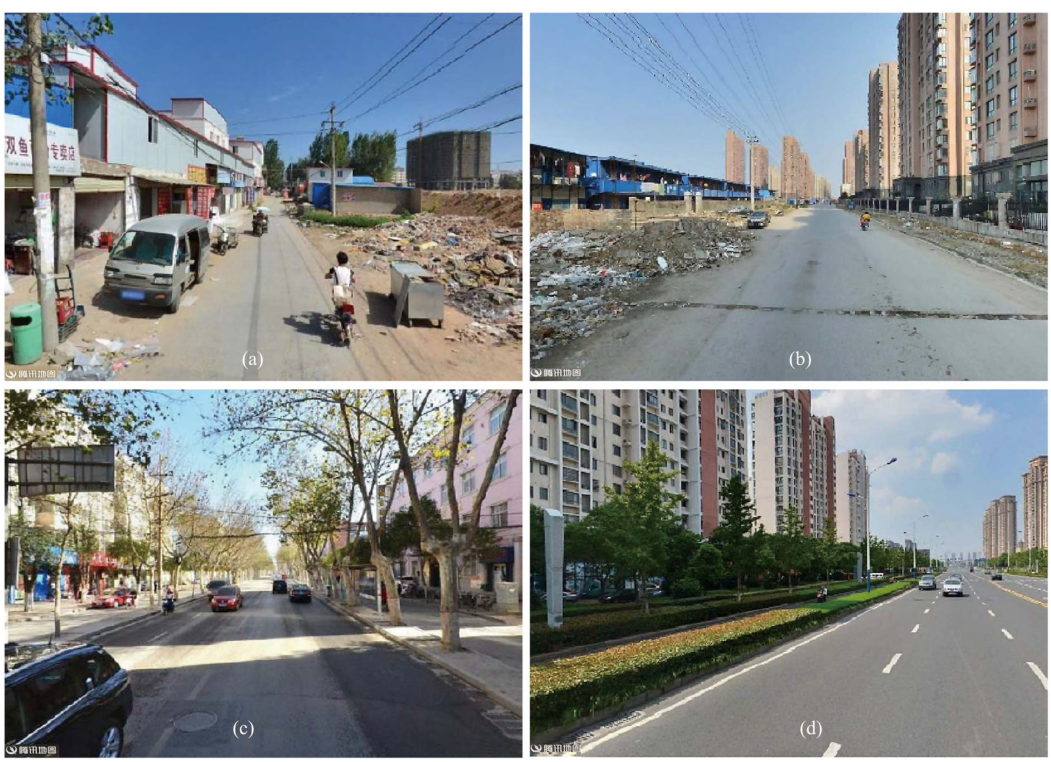

Figure 4. Comparison of street view images with different levels of physical disorder of streets. (A) Maximum (0.836) physical disorder score, Fushun. (B) Upper quartile (0.396) physical disorder score, Wuhu. (C) Mean (0.214) physical disorder score, Wuhan. (D) Minimum (0) physical disorder score, Changzhou. Data from Tencent Street View images in 2015.

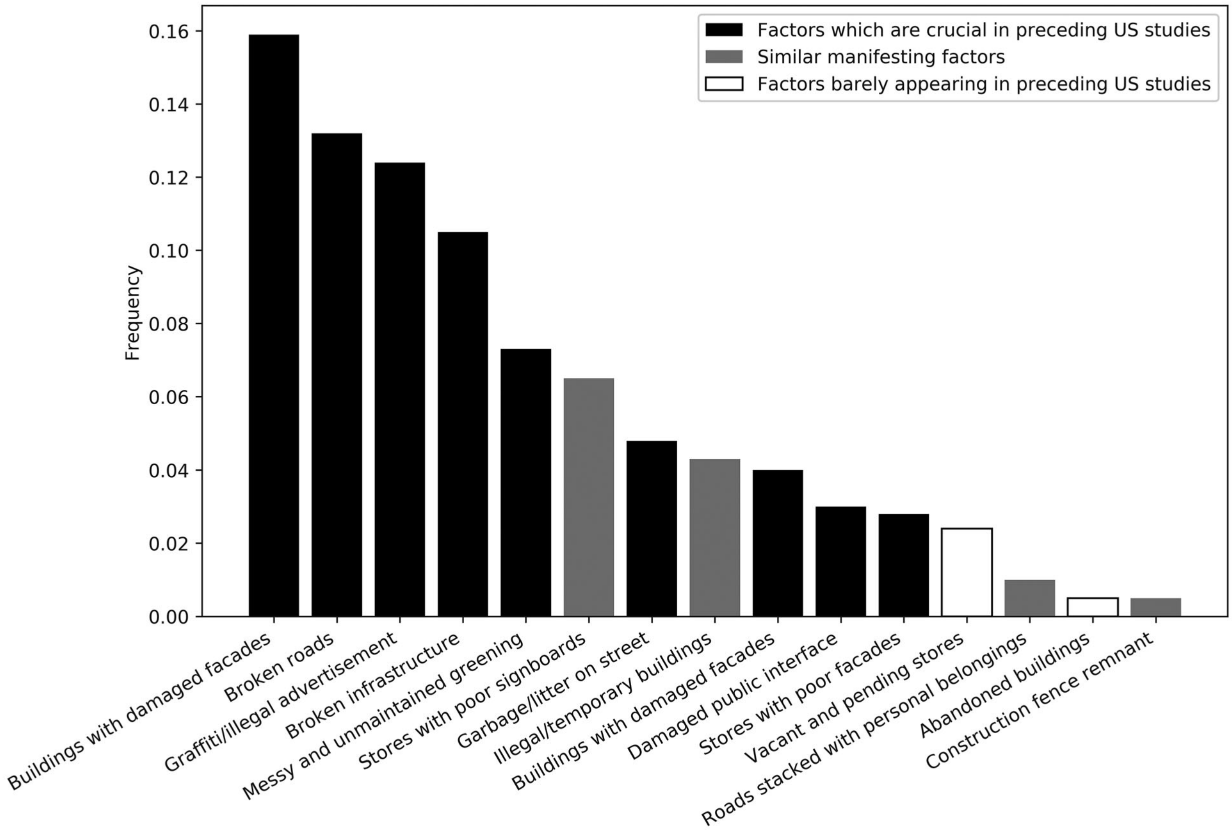

Figure 5. Average physical disorder probability of fifteen factors.

Table 3. Regression results of physical disorder and street attributes (with control variables)

	Physical disorder	
Variables	p value	Standardized beta
Street length	0.000***	0.4608
Street function density	0.000***	–0.0271
Street function mix	0.000***	0.2424
Street junction density	0.08*	–0.0143
Distance to the city center	0.05**	0.3382
Observations	769,407	
R^2	0.413	

*$p < 0.1$.
**$p < 0.05$.
***$p < 0.01$.

factors, buildings with damaged facades, broken roads, graffiti or illegal advertisement, and broken infrastructure are the main manifestations of street physical disorder in Chinese cities, with relatively higher disorder probabilities of 0.159, 0.134, 0.129, and 0.113, respectively.

After finding the predicted results of street physical disorder in 264 Chinese cities, we found it a great opportunity to further explore the influencing factors of physical disorder, because we have such a large sample size, which also represents the whole Chinese urban system. In accordance with the literature, we selected five variables that represent street space attributes, including street length, function density, function mix, junction density, and distance to the city center, and then used a linear regression model to analyze the association between street variables and the streets' physical disorder score (Table 3).

The regression results show that the disorder probability of street space has positive correlations with the street length, function mix, and distance to the city center and negative correlations with the street function density and junction density. In other words, our results indicate that longer and more diverse streets, or those closer to the city center, might contain more disorder factors, thus leading to a greater probability of disorder occurrence. Streets with more points of interest and intersections are found to have a lower level of physical disorder. By calculating the average score for each street segment, we developed scoring maps for the physical disorder at the city level (Figure 6). The study labeled the top 5

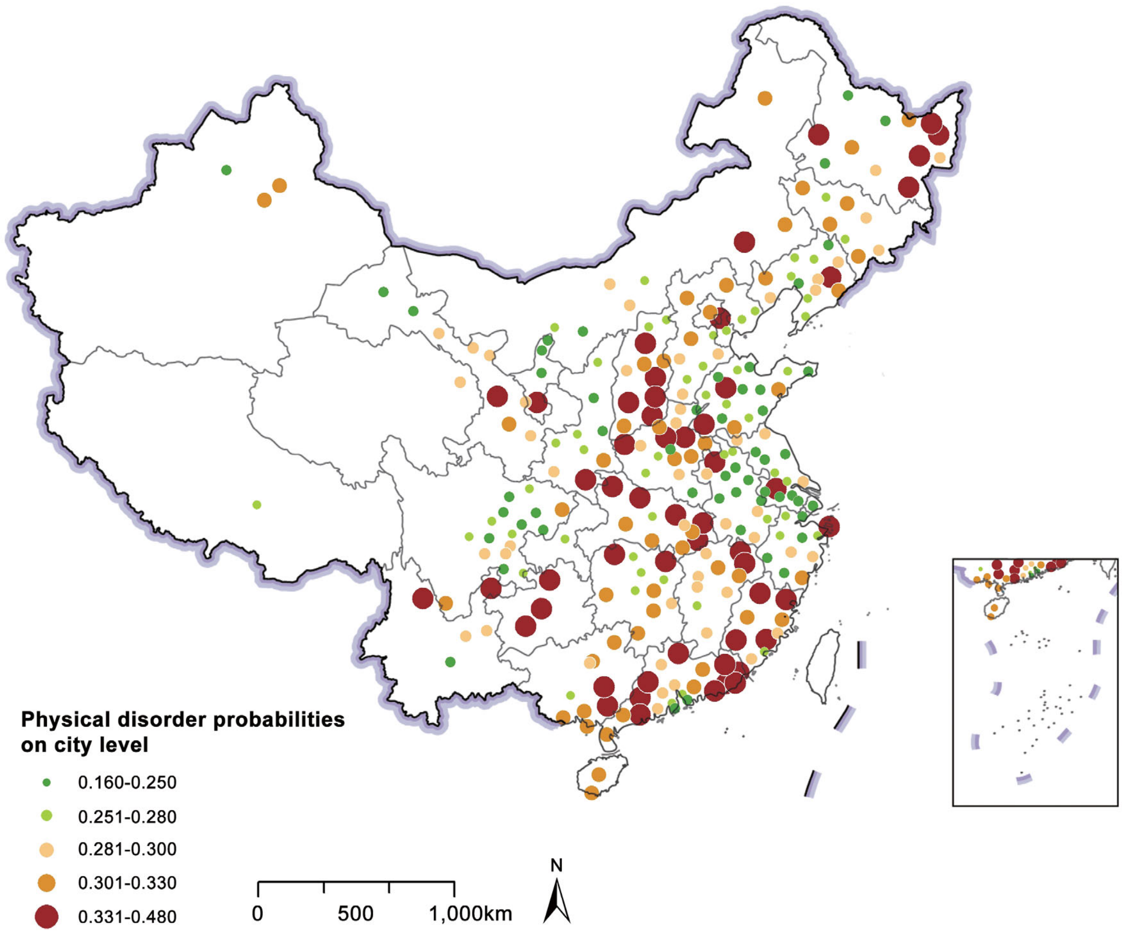

Figure 6. Spatial distribution of cities with different physical disorder probabilities.

percent of streets with the highest probability of physical disorder among all sampled streets across the country. These spaces with a higher probability of physical disorder are evenly and widely distributed across the city without apparent spatial aggregation. Consistent with our findings, however, these streets are generally distributed in areas far from the city center. In addition, compared to urban centers, due to low housing prices, large numbers of urban villages and old residential areas are located in regions far from downtown, where residents are less concerned about spatial quality.

City Level: Physical Disorder Maps of Street Space in China

We used Jenks natural breaks to divide the disorder probability of cities into five categories and then labeled the cities with disorder probabilities higher than 0.33 as the most disordered category (see Figure 6, and full city list in Appendix). The most disordered cities are scattered across the country, such as in the northern region of China, and exist in central cities as well as southern cities. Cities with better urban environments (i.e., lower physical disorder scores) are located in western regions and eastern China, which are scenic landscapes, or the highly developed coastal Yangtze River Delta region.

Regarding the spatial distribution of physical disorder at the city scale, although the most urban physical disorder is relatively scattered within the city, the physical disorder hot spots reveal three typical patterns of distribution in most cities: (a) scattered (109 out of 264), (b) diffused along the urban expansion direction (89 out of 264), and (c) linear concentrated along arterial roads (42 out of 264). Twenty-four cities combined Characteristics b and c (see Figure 7).

a. For these scattered cities, some are low-administrative-level ones with a small overall spatial scale and relatively simple road network, and

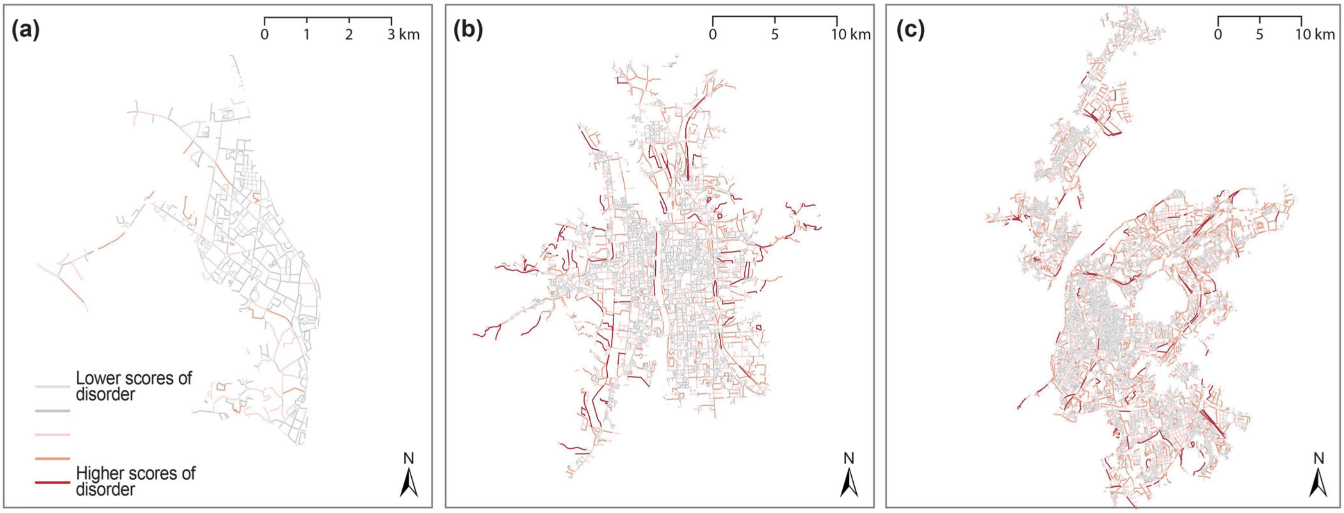

Figure 7. Physical disorder hot spots exhibit three spatial distribution patterns. (A) Scattered: Leshan; (B) diffused along the urban expansion direction: Taiyuan; (C) linear aggregation along arterial roads: Nanjing.

some are tourist cities, leading to a better overall street environment due to better construction and maintenance (e.g., Leshan).

b. For most medium-sized cities, which are facing rapid urban expansion with limited urban resources, it leads to urban expansion in the peripheral areas, mostly urban–rural junctions or urban suburbs to be developed, showing a diffused distribution of physical disorder, with more nonurban landscapes such as farmland and countryside (e.g., Taiyuan).
c. The third pattern refers to cities where the overall physical disorder is moderate, and places with a high probability of physical disorder are linearly distributed along the arterial roads, especially the common but poorly maintained wide roads, expressways, and so on. In addition, some provincial capital cities or large cities also show the characteristics of linear concentration along the arterial roads and polycentric spatial type, which are consistent with the existing multicentered urban structure (e.g., Nanjing).

Even with the existence of the aforementioned spatial distribution patterns, however, the dominant factor contributing to the spatial quality of each city varies, which deserves further research.

Conclusions and Discussion

Concluding Remarks

This article proposes an approach combining a deep learning algorithm and SVIs to quantitatively measure the physical disorder of urban street spaces. Fifteen physical disorder factors in five categories—architectural, commercial, road, greening, and other infrastructure aspects—were defined and manually annotated in the training SVI set. The pretrained MobileNet V3 model performed well, with an average accuracy of 72.77 percent. To further test the approach, a case study was conducted in 264 Chinese cities. Based on the prediction results of the deep learning model, the study developed a series of maps showing the physical disorder of urban street spaces in Chinese cities and revealed significant patterns of these phenomena at both the street and city scales. At the street level, (1) physical disorder is commonly seen in the street spaces of Chinese cities, although the spatial quality remains moderate for most streets; (2) the low spatial quality in architecture, roads, and commerce is the main manifestation of the street space disorder in China; and (3) street length, functional diversity, and distance from the city center are all found to be positively associated with physical disorder of a street. At the city scale, physical disorder of street spaces exhibits three spatial patterns: monocentric, linear concentration along arterial roads, and polycentric distribution across the city.

Discussion

In terms of the contribution of this article, we found several areas in which our study makes a significant contribution. First, the attention to physical disorder has experienced quick growth during the past ten years, according to our keyword search on Google Scholar, but theories (e.g., mechanism and the externalities of physical disorder), measurement (e.g., conventional manual audit or questionnaire), and empirical analysis (limited case cities) all face limitations in the existing literature. Our study has clear goals to enrich the related research and to overcome these limitations. Second, our innovative approach to quantifying physical disorder with SVIs and deep learning not only overcomes the limitations of the conventional auditing and field survey, but also provides a universal tool that can easily be applied to almost any place in the world, for large-scale analysis at a lower cost. Third, such a large-scale empirical analysis that includes most urban areas in China, which represent the Chinese urban system, gives us valuable information to understand the characteristics (e.g., degree, spatial distribution) of the physical disorder at different scales, and enables us to reveal the mechanisms behind the appearance of physical disorder. All of these factors help us learn more about physical disorder and enrich the theories in urban space.

In practice, by identifying the physical disorder in urban street spaces in a large number of cities, as well as providing the visualization maps for each city, we believe this article could assist local governments in evaluating the street space quality of their cities, and especially help them to identify the existing problems that cause the physical disorder in specific streets, which might have already imposed negative externalities, such as decreased rent and urban vitality and increased stress and crime. The combination of the SVI data and deep learning also sheds light on a more comprehensive understanding of the urban built environment at multiple scales including location, street, and city, which provides refined support for policymaking in projects, such as urban renewal, street revitalization, and community development, thus helping improve the overall quality of life. In addition, local residents could also benefit from these physical disorder maps by learning more about their surrounding urban spaces and better engaging in improving them or adjusting their behaviors and location choice.

Notably, there are also a few limitations worth further discussion in the near future. First, the SVIs have spatial and temporal limitations; spatially they lack data on inaccessible local backroads and alleys. In addition, street views generally cover only central urban areas (i.e., densely populated areas). Temporally, commercial street views are slow to update and urban renewal is not reflected in a timely manner. For example, Tencent Street View images have not been updated since 2015. In the near future, we will be able to access more SVI data from Baidu Maps, which is another major map service company in China, to further expand our study. Another alternative is an active urban sensing strategy that could help alleviate this problem by hiring self-employed agents, such as vehicles, bicycles, and pedestrians to collect street views. Second, using the binary indicator in identifying physical disorder has its limitations, such as one single abandoned building on the street must have a different physical disorder effect than a row of abandoned buildings. In this pilot study, though, we were attempting to first answer the question of whether physical disorder exists in urban street spaces but paid little attention to how much disorder the streets are in. The future plan could be implemented with the SegNet model, which is also a deep learning algorithm that enables us to not only identify the physical disorder factors' existence, but also to know the area proportion of each factor, such as the area of the unkempt facades or graffiti, and how many street vendors can be seen. Image segmentation model annotation, however, needs to depict the shape of each object resulting in a huge workload, so it still faces a huge challenge due to the lack of a large-scale annotation database.

Acknowledgment

The data and code of this study are available at Mendeley Data (http://dx.doi.org/10.17632/d3d4h5bvss.1).

Funding

This work was supported by the National Natural Science Foundation of China [No. 52178044, 71834005 and No. 51878052].

Supplemental Material

Supplemental data for this article can be accessed on the publisher's site at: https://doi.org/10.1080/24694452.2022.2114417

The auditing guidance of this study is available as supplemental material. It will help readers to understand how the auditors identify the physical disorder in the process of virtual auditing. It also provides guidance for the research community in replicating the approach in future studies on physical disorder in other cities.

ORCID

Jingjia Chen http://orcid.org/0000-0002-8220-6330
Long Chen http://orcid.org/0000-0002-0972-449X
Yan Li http://orcid.org/0000-0001-6650-7726
Wenjia Zhang http://orcid.org/0000-0002-7211-4205
Ying Long http://orcid.org/0000-0002-8657-6988

Note

1. The prefecture is the basic administrative unit between province and county in China, and there are 293 prefectural cities in total until 2021 (National Bureau of Statics of China; https://data.stats.gov.cn/easyquery.htm?cn=C01). Therefore, these cities represent the most densely populated and rapidly developing urbanization regions in China.

References

Bader, M. D. M., S. J. Mooney, B. Bennett, and A. G. Rundle. 2017. The promise, practicalities, and perils of virtually auditing neighborhoods using Google Street View. *The Annals of the American Academy of Political and Social Science* 669 (1):18–40. doi: 10.1177/0002716216681488.

Burdette, A. M., and T. D. Hill. 2008. An examination of processes linking perceived neighborhood disorder and obesity. *Social Science & Medicine* 67 (1):38–46.

Clarke, P., J. Ailshire, R. Melendez, M. Bader, and J. Morenoff. 2010. Using Google Earth to conduct a neighborhood audit: Reliability of a virtual audit instrument. *Health & Place* 16 (6):1224–29.

Day, K., M. Boarnet, M. Alfonzo, and A. Forsyth. 2006. The Irvine-Minnesota inventory to measure built environments. *American Journal of Preventive Medicine* 30 (2):144–52. doi: 10.1016/j.amepre.2005.09.017.

Franzini, L., M. O. Caughy, S. M. Nettles, and P. O'Campo. 2008. Perceptions of disorder: Contributions of neighborhood characteristics to subjective perceptions of disorder. *Journal of Environmental Psychology* 28 (1):83–93. doi: 10.1016/j.jenvp.2007.08.003.

Grubesic, T. H., D. Wallace, A. W. Chamberlain, and J. R. Nelson. 2018. Using unmanned aerial systems (UAS) for remotely sensing physical disorder in neighborhoods. *Landscape and Urban Planning* 169:148–59.

Helbich, M., Y. Yao, Y. Liu, J. Zhang, P. Liu, and R. Wang. 2019. Using deep learning to examine street view green and blue spaces and their associations with geriatric depression in Beijing, China. *Environment International* 126:107–17. doi: 10.1016/j.envint.2019.02.013.

Howard, A., M. Sandler, B. Chen, W. Wang, L.-C. Chen, M. Tan, G. Chu, V. Vasudevan, Y. Zhu, R. Pang, et al. 2019. Searching for MobileNetV3. In *Proceedings of the IEEE/CVF International Conference on Computer Vision*, 1314–24. https://ieeexplore.ieee.org/xpl/conhome/8972782/proceeding

Jiang, B., C. N. S. Mak, H. Zhong, L. Larsen, and C. J. Webster. 2018. From broken windows to perceived routine activities: Examining impacts of environmental interventions on perceived safety of urban alleys. *Frontiers in Psychology* 9:2450.

Jones, M., A. R. Pebley, and N. Sastry. 2011. Eyes on the block: Measuring urban physical disorder through in-person observation. *Social Science Research* 40 (2):523–37.

Kendall, A., V. Badrinarayanan, and R. Cipolla. 2015. Bayesian SegNet: Model uncertainty in deep convolutional encoder–decoder architectures for scene understanding. *arXiv Preprint* 1511.02680.

Keralis, J. M., M. Javanmardi, S. Khanna, P. Dwivedi, D. Huang, T. Tasdizen, and Q. C. Nguyen. 2020. Health and the built environment in United States cities: Measuring associations using Google Street View-derived indicators of the built environment. *BMC Public Health* 20 (1):1–10. doi: 10.1186/s12889-020-8300-1.

Keyes, K. M., K. A. McLaughlin, K. C. Koenen, E. Goldmann, M. Uddin, and S. Galea. 2012. Child maltreatment increases sensitivity to adverse social contexts: Neighborhood physical disorder and incident binge drinking in Detroit. *Drug and Alcohol Dependence* 122 (1–2):77–85.

Landis, J. R., and G. G. Koch. 1977. The measurement of observer agreement for categorical data. *Biometrics* 33 (1):159–74. doi: 10.2307/2529310.

Li, W., Y. Long, M. P. Kwan, N. Liu, Y. Li, and Y. Zhang. 2022. Measuring individuals' mobility-based exposure to neighborhood physical disorder with wearable cameras. *Applied Geography* 145:102728. doi: 10.1016/j.apgeog.2022.102728.

Ma, S., and Y. Long. 2020. Functional urban area delineations of cities on the Chinese mainland using massive Didi ride-hailing records. *Cities* 97:102532. doi: 10.1016/j.cities.2019.102532.

Mayne, S. L., B. F. Pellissier, and K. N. Kershaw. 2019. Neighborhood physical disorder and adverse pregnancy outcomes among women in Chicago: A cross-sectional analysis of electronic health record data. *Journal of Urban Health: Bulletin of the New York Academy of Medicine* 96 (6):823–34.

Mooney, S. J., M. D. M. Bader, G. S. Lovasi, K. M. Neckerman, J. O. Teitler, and A. G. Rundle. 2014. Validity of an ecometric neighborhood physical disorder measure constructed by virtual street audit. *American Journal of Epidemiology* 180 (6):626–35.

Mooney, S. J., C. J. DiMaggio, G. S. Lovasi, K. M. Neckerman, M. D. Bader, J. O. Teitler, ... and A. G. Rundle. 2016. Use of Google Street View to assess environmental contributions to pedestrian injury. *American Journal of Public Health* 106 (3):462–69.

Naik, N., J. Philipoom, R. Raskar, and C. Hidalgo. 2014. Streetscore—Predicting the perceived safety of one million streetscapes. Paper presented at the 27th IEEE Conference on Computer Vision and Pattern Recognition (CVPR), Columbus, OH, June 23–28.

Nguyen, Q. C., Y. Huang, A. Kumar, H. Duan, J. M. Keralis, P. Dwivedi, H.-W. Meng, K. D. Brunisholz, J. Jay, M. Javanmardi, et al. 2020. Using 164 million Google Street View images to derive built environment predictors of COVID-19 cases. *International Journal of Environmental Research and Public Health* 17 (17):6359. doi: 10.3390/ijerph17176359.

Perkins, D. D., J. W. Meeks, and R. B. Taylor. 1992. The physical environment of street blocks and resident perceptions of crime and disorder: Implications for theory and measurement. *Journal of Environmental Psychology* 12 (1):21–34. doi: 10.1016/S0272-4944(05)80294-4.

Quinn, J. W., S. J. Mooney, D. M. Sheehan, J. O. Teitler, K. M. Neckerman, T. K. Kaufman, G. S. Lovasi, D. M. Michael, and B. A. G. Rundle. 2016. Neighborhood physical disorder in New York City. *Journal of Maps* 12 (1):53–60.

Ross, C. E., and S. J. Jang. 2000. Neighborhood disorder, fear, and mistrust: The buffering role of social ties with neighbors. *American Journal of Community Psychology* 28 (4):401–20.

Sampson, R. J., and S. W. Raudenbush. 1999. Systematic social observation of public spaces: A new look at disorder in urban neighborhoods. *American Journal of Sociology* 105 (3):603–51. doi: 10.1086/210356.

Shen, Q. M., W. Zeng, Y. Ye, S. M. Arisona, S. Schubiger, R. Burkhard, and H. Qu. 2018. StreetVizor: Visual exploration of human-scale urban forms based on street views. *IEEE Transactions on Visualization and Computer Graphics* 24 (1):1004–13.

Skogan, W. G. 1990. *Disorder and decline: Crime and the spiral of decay in American cities*. New York: The Free Press.

Suel, E., J. W. Polak, J. E. Bennett, and M. Ezzati. 2019. Measuring social, environmental and health inequalities using deep learning and street imagery. *Scientific Reports* 9 (1):1–10.

Tang, J., and Y. Long. 2019. Measuring visual quality of street space and its temporal variation: Methodology and its application in the Hutong area in Beijing. *Landscape and Urban Planning* 191:103436.

Taylor, R. B., S. A. Shumaker, and S. D. Gottfredson. 1985. Neighborhood-level links between physical features and local sentiments: Deterioration, fear of crime, and confidence. *Journal of Architectural and Planning Research* 2 (4):261–75.

Vanwolleghem, G., A. Ghekiere, G. Cardon, I. De Bourdeaudhuij, S. D'Haese, C. M. Geremia, ... and D. Van Dyck. 2016. Using an audit tool (MAPS Global) to assess the characteristics of the physical environment related to walking for transport in youth: Reliability of Belgian data. *International Journal of Health Geographics* 15 (1):1–11.

Ye, Y., D. Richards, Y. Lu, X. Song, Y. Zhuang, W. Zeng, and T. Zhong. 2019. Measuring daily accessed street greenery: A human-scale approach for informing better urban planning practices. *Landscape and Urban Planning* 191:103434.

Zhang, F., B. L. Zhou, L. Liu, Y. Liu, H. H. Fung, H. Lin, and C. Ratti. 2018. Measuring human perceptions of a large-scale urban region using machine learning. *Landscape and Urban Planning* 180:148–60. doi: 10.1016/j.landurbplan.2018.08.020.

Zhang, Z., Y. Long, L. Chen, and C. Chen. 2021. Assessing personal exposure to urban greenery using wearable cameras and machine learning. *Cities* 109:103006. doi: 10.1016/j.cities.2020.103006.

JINGJIA CHEN has earned both a master's and a bachelor's degree from the Department of Urban Planning, Tsinghua University, Beijing, China, 100084. E-mail:chen-jj18@tsinghua.org.cn. Her research interests include urban big data analysis and urban design for future cities.

LONG CHEN is a Lecturer in the Faculty of Architecture, Civil and Transportation Engineering, Beijing University of Technology, Beijing, China, 100124. E-mail: lchen@bjut.edu.cn. His research interests include transportation big data analysis and sustainable transportation.

YAN LI is a Research Fellow in the Department of Urban Planning at Tsinghua University, Beijing, China 100084. E-mail: yanli427@hotmail.com. Her research interests include geographic information systems, human dynamics, and urban science.

WENJIA ZHANG is an Assistant Professor in the School of Urban Planning & Design, Peking University Shenzhen Graduate School, Shenzhen, Guangdong, China, 518055. E-mail: zhangwj@pkusz.edu.cn. His research interests include network complexity in urban and geography studies, network and spatial economics, land use and transportation planning, as well as big data and machine learning approaches.

YING LONG is an Associate Professor in the Department of Urban Planning, Tsinghua University, Beijing, China, 100084. E-mail: ylong@tsinghua.edu.cn. His research interests include (new) urban science, urban big data analysis, urban modeling, data enhanced design, smart cities, and future cities.

Appendix. Physical disorder probabilities and the city-scale spatial distribution patterns for 264 cities

City	Spatial distribution pattern	Physical disorder probabilities
Ankang	(b) Diffused along the urban expansion direction	0.02467
Anqing	(c) Linear concentrated along arterial roads	0.02646
Anshun	(a) Scattered	0.02647
Anyang	(c) Linear concentrated along arterial roads	0.03116
Anshan	(b) Diffused along the urban expansion direction	0.02166
Bayannur	(a) Scattered	0.03206
Bazhong	(a) Scattered	0.02214
Baicheng	(b) Diffused along the urban expansion direction	0.02586
Baishan	(b) Diffused along the urban expansion direction	0.02090
Baiyin	(b) Diffused along the urban expansion direction	0.02516
Baise	(a) Scattered	0.02329
Bengbu	(c) Linear concentrated along arterial roads	0.02958
Baotou	(b) Diffused along the urban expansion direction	0.02550
Baoji	(b) Diffused along the urban expansion direction	0.02731
Baoding	(a) Scattered	0.02983
Baoshan	(a) Scattered	0.02020
Beijing	Cities that combine the (b) and (c) characteristics	0.03164
Benxi	(b) Diffused along the urban expansion direction	0.02964
Bozhou	(a) Scattered	0.02904
Changde	(a) Scattered	0.02139
Changzhou	(c) Linear concentrated along arterial roads	0.02556
Chaoyang	(b) Diffused along the urban expansion direction	0.02508
Chaozhou	(a) Scattered	0.02523
Chenzhou	(b) Diffused along the urban expansion direction	0.02793
Chengdu	(c) Linear concentrated along arterial roads	0.02153
Chengde	(a) Scattered	0.02901
Chizhou	(a) Scattered	0.02307
Chifeng	(b) Diffused along the urban expansion direction	0.03215
Chongzuo	(b) Diffused along the urban expansion direction	0.03157
Chuzhou	(c) Linear concentrated along arterial roads	0.02903
Dazhou	(b) Diffused along the urban expansion direction	0.02043
Dalian	(c) Linear concentrated along arterial roads	0.02067
Daqing	(c) Linear concentrated along arterial roads	0.02587
Datong	(c) Linear concentrated along arterial roads	0.03341
Dandong	(b) Diffused along the urban expansion direction	0.04420
Deyang	(a) Scattered	0.02186
Dezhou	(c) Linear concentrated along arterial roads	0.03091
Dingxi	(c) Linear concentrated along arterial roads	0.02997
Dongguan	(a) Scattered	0.02234
Dongying	(a) Scattered	0.02514
Erdos	(a) Scattered	0.02394
Ezhou	(c) Linear concentrated along arterial roads	0.02562
Foshan	(a) Scattered	0.02006
Fu2zhou	(a) Scattered	0.02295
Fushun	Cities that combine the (b) and (c) characteristics	0.02672
Fu3zhou	(a) Scattered	0.02775
Fuxin	Cities that combine the (b) and (c) characteristics	0.02742
Fuyang	(c) Linear concentrated along arterial roads	0.03753
Ganzhou	(a) Scattered	0.02371
Guyuan	(a) Scattered	0.02583
Guangan	(b) Diffused along the urban expansion direction	0.01768
Guangyuan	(b) Diffused along the urban expansion direction	0.02290
Guangzhou	(c) Linear concentrated along arterial roads	0.02258

(*Continued*)

Appendix. (*Continued*).

City	Spatial distribution pattern	Physical disorder probabilities
Guigang	(c) Linear concentrated along arterial roads	0.02322
Guiyang	(b) Diffused along the urban expansion direction	0.02598
Guilin	Cities that combine the (b) and (c) characteristics	0.02536
Harbin	(b) Diffused along the urban expansion direction	0.02098
Haikou	(a) Scattered	0.02361
Handan	(b) Diffused along the urban expansion direction	0.02977
Hanzhong	(a) Scattered	0.02202
Hangzhou	(a) Scattered	0.01953
Hefei	(a) Scattered	0.02554
Hechi	(c) Linear concentrated along arterial roads	0.02506
Heyuan	(b) Diffused along the urban expansion direction	0.02045
Heze	(a) Scattered	0.03816
Hezhou	(a) Scattered	0.01935
Hebi	(b) Diffused along the urban expansion direction	0.03971
Hegang	Cities that combine the (b) and (c) characteristics	0.03981
Heihe	(b) Diffused along the urban expansion direction	0.02657
Hengshui	(b) Diffused along the urban expansion direction	0.03356
Hengyang	Cities that combine the (b) and (c) characteristics	0.02603
Hohhot	(c) Linear concentrated along arterial roads	0.02664
Hulunbuir	(b) Diffused along the urban expansion direction	0.02998
Huludao	(b) Diffused along the urban expansion direction	0.02216
Huzhou	(a) Scattered	0.02018
Huaihua	(c) Linear concentrated along arterial roads	0.02627
Huaian	(b) Diffused along the urban expansion direction	0.03232
Huaibei	(a) Scattered	0.02996
Huanggang	(a) Scattered	0.02647
Huangshan	(a) Scattered	0.02111
Huangshi	(a) Scattered	0.02515
Huizhou	Cities that combine the (b) and (c) characteristics	0.02202
Jixi	Cities that combine the (b) and (c) characteristics	0.03549
Ji'an	(a) Scattered	0.02197
Jilin	Cities that combine the (b) and (c) characteristics	0.02356
Ji'nan	(b) Diffused along the urban expansion direction	0.02793
Ji'ning	(b) Diffused along the urban expansion direction	0.03573
Jiamusi	Cities that combine the (b) and (c) characteristics	0.02520
Jiaxing	(b) Diffused along the urban expansion direction	0.02135
Jiayuguan	Cities that combine the (b) and (c) characteristics	0.02655
Jiangmen	(a) Scattered	0.02252
Jiaozuo	(a) Scattered	0.03057
Jieyang	(a) Scattered	0.02060
Jinchang	Cities that combine the (b) and (c) characteristics	0.02427
Jinhua	(a) Scattered	0.01783
Jinzhou	(c) Linear concentrated along arterial roads	0.02755
Jincheng	(b) Diffused along the urban expansion direction	0.03011
Jinzhong	Cities that combine the (b) and (c) characteristics	0.03313
Jinmen	(a) Scattered	0.02618
Jingzhou	(a) Scattered	0.02678
Jingdezhen	(c) Linear concentrated along arterial roads	0.02769
Jiujiang	(a) Scattered	0.02338
Jiuquan	(a) Scattered	0.02200
Kaifeng	(b) Diffused along the urban expansion direction	0.02575
Kunming	(a) Scattered	0.02154
Lhasa	(c) Linear concentrated along arterial roads	0.02616
Laibin	(b) Diffused along the urban expansion direction	0.02654
Laiwu	(b) Diffused along the urban expansion direction	0.03453

(*Continued*)

Appendix. (*Continued*).

City	Spatial distribution pattern	Physical disorder probabilities
Lanzhou	Cities that combine the (b) and (c) characteristics	0.02544
Langfang	(a) Scattered	0.02768
Leshan	(a) Scattered	0.01811
Lijiang	(a) Scattered	0.01630
Lishui	(a) Scattered	0.01806
Lianyungang	(b) Diffused along the urban expansion direction	0.02798
Liaoyang	(b) Diffused along the urban expansion direction	0.02520
Liaoyuan	(b) Diffused along the urban expansion direction	0.02674
Liaocheng	(b) Diffused along the urban expansion direction	0.03362
Linfen	(a) Scattered	0.02975
Linyi	(b) Diffused along the urban expansion direction	0.04503
Liuzhou	Cities that combine the (b) and (c) characteristics	0.02656
Lu'an	(a) Scattered	0.02956
Liupanshui	(b) Diffused along the urban expansion direction	0.02903
Longyan	(b) Diffused along the urban expansion direction	0.03168
Longnan	(b) Diffused along the urban expansion direction	0.02090
Loudi	(a) Scattered	0.03026
Luzhou	(a) Scattered	0.01846
Luoyang	(b) Diffused along the urban expansion direction	0.02660
Lvliang	(b) Diffused along the urban expansion direction	0.03135
Maanshan	(b) Diffused along the urban expansion direction	0.03096
Maoming	(b) Diffused along the urban expansion direction	0.02193
Meishan	(b) Diffused along the urban expansion direction	0.01811
Mianyang	(b) Diffused along the urban expansion direction	0.02061
Mudanjiang	(c) Linear concentrated along arterial roads	0.02331
Nanchang	(c) Linear concentrated along arterial roads	0.02299
Nanchong	(b) Diffused along the urban expansion direction	0.02235
Nanjing	(c) Linear concentrated along arterial roads	0.02668
Nanning	(a) Scattered	0.02542
Nanping	(c) Linear concentrated along arterial roads	0.02430
Nantong	(a) Scattered	0.02826
Nanyang	(b) Diffused along the urban expansion direction	0.03665
Neijiang	(a) Scattered	0.02339
Ningbo	(a) Scattered	0.02158
Ningde	(a) Scattered	0.02406
Panzhihua	(c) Linear concentrated along arterial roads	0.03009
Panjin	(c) Linear concentrated along arterial roads	0.02771
Pingdingshan	Cities that combine the (b) and (c) characteristics	0.04009
Pingxiang	(c) Linear concentrated along arterial roads	0.02486
Putian	(a) Scattered	0.01868
Puyang	(b) Diffused along the urban expansion direction	0.03296
Qitaihe	(b) Diffused along the urban expansion direction	0.03327
Qiqihar	(b) Diffused along the urban expansion direction	0.02506
Qinzhou	(a) Scattered	0.01950
Qinhuangdao	(b) Diffused along the urban expansion direction	0.02983
Qingdao	(a) Scattered	0.02292
Qingyuan	(b) Diffused along the urban expansion direction	0.02040
Qingyang	(a) Scattered	0.02374
Quzhou	(b) Diffused along the urban expansion direction	0.02605
Quanzhou	(a) Scattered	0.02268
Rizhao	(c) Linear concentrated along arterial roads	0.02837
Sanmenxia	(b) Diffused along the urban expansion direction	0.03839
Sanming	(a) Scattered	0.02464
Sanya	(a) Scattered	0.02332
Xiamen	(a) Scattered	0.01896

(*Continued*)

Appendix. (*Continued*).

City	Spatial distribution pattern	Physical disorder probabilities
Shantou	(b) Diffused along the urban expansion direction	0.02168
Shanwei	(a) Scattered	0.02059
Shangqiu	(b) Diffused along the urban expansion direction	0.03472
Shanghai	(b) Diffused along the urban expansion direction	0.02160
Shangrao	(a) Scattered	0.02231
Shaoguan	(a) Scattered	0.02723
Shaoyang	(b) Diffused along the urban expansion direction	0.02477
Shaoxing	(b) Diffused along the urban expansion direction	0.02389
Shenzhen	(c) Linear concentrated along arterial roads	0.02312
Shenyang	Cities that combine the (b) and (c) characteristics	0.02261
Shiyan	(a) Scattered	0.02661
Shijiazhuang	Cities that combine the (b) and (c) characteristics	0.02643
Shizuishan	(a) Scattered	0.02352
Shuangyashan	(b) Diffused along the urban expansion direction	0.02767
Shuozhou	(a) Scattered	0.03088
Siping	Cities that combine the (b) and (c) characteristics	0.02705
Songyuan	(b) Diffused along the urban expansion direction	0.02338
Su1zhou	(c) Linear concentrated along arterial roads	0.02736
Suihua	(b) Diffused along the urban expansion direction	0.02453
Suizhou	(a) Scattered	0.02935
Suining	(a) Scattered	0.02176
Taizhou	(a) Scattered	0.01819
Taiyuan	(b) Diffused along the urban expansion direction	0.02809
Taian	(b) Diffused along the urban expansion direction	0.03183
Taizhou	(a) Scattered	0.02746
Tangshan	Cities that combine the (b) and (c) characteristics	0.02787
Tianjin	(c) Linear concentrated along arterial roads	0.02526
Tianshui	(a) Scattered	0.02711
Tonghua	(c) Linear concentrated along arterial roads	0.02461
Tongliao	(b) Diffused along the urban expansion direction	0.02933
Tongchuan	(b) Diffused along the urban expansion direction	0.02774
Weihai	(a) Scattered	0.02632
Weifang	(b) Diffused along the urban expansion direction	0.02700
Wenzhou	(a) Scattered	0.02003
Wuhai	(a) Scattered	0.02808
Ulanqab	(b) Diffused along the urban expansion direction	0.03420
Urumqi	Cities that combine the (b) and (c) characteristics	0.02572
Wuxi	Cities that combine the (b) and (c) characteristics	0.02419
Wuzhong	(a) Scattered	0.02388
Wuzhou	(a) Scattered	0.02414
Wuhan	(c) Linear concentrated along arterial roads	0.02231
Wuwei	(a) Scattered	0.02683
Xi'an	(c) Linear concentrated along arterial roads	0.02530
Xi'ning	(b) Diffused along the urban expansion direction	0.02448
Xianning	(a) Scattered	0.02646
Xianyang	(a) Scattered	0.02563
Xiangtan	(b) Diffused along the urban expansion direction	0.02780
Xiaogan	(a) Scattered	0.02373
Xinzhou	(b) Diffused along the urban expansion direction	0.02828
Xinxiang	(a) Scattered	0.02989
Xinyu	(b) Diffused along the urban expansion direction	0.02941
Xinyang	(c) Linear concentrated along arterial roads	0.03882
Xingtai	(a) Scattered	0.02967
Suqian	(a) Scattered	0.03246
Xuzhou	(c) Linear concentrated along arterial roads	0.03105

(*Continued*)

Appendix. (*Continued*).

City	Spatial distribution pattern	Physical disorder probabilities
Xuchang	(c) Linear concentrated along arterial roads	0.02952
Xuanzhou	(a) Scattered	0.02766
Ya'an	(a) Scattered	0.02510
Yantai	(a) Scattered	0.02944
Yanan	(a) Scattered	0.01802
Yancheng	(a) Scattered	0.02728
Yangzhou	(a) Scattered	0.02547
Yangquan	(c) Linear concentrated along arterial roads	0.03684
Yichun	(b) Diffused along the urban expansion direction	0.02543
Yibin	(b) Diffused along the urban expansion direction	0.02090
Yichang	(a) Scattered	0.02531
Yichun	(a) Scattered	0.02446
Yiyang	(a) Scattered	0.02541
Yinchuan	(a) Scattered	0.02438
Yingtan	(b) Diffused along the urban expansion direction	0.02870
Yingkou	(b) Diffused along the urban expansion direction	0.02639
Yongzhou	(b) Diffused along the urban expansion direction	0.02765
Yu4lin	(b) Diffused along the urban expansion direction	0.02606
Yuxi	(b) Diffused along the urban expansion direction	0.01825
Yueyang	(b) Diffused along the urban expansion direction	0.02988
Yunfu	(b) Diffused along the urban expansion direction	0.01877
Yuncheng	Cities that combine the (b) and (c) characteristics	0.02419
Zaozhuang	(a) Scattered	0.03721
Zhanjiang	(a) Scattered	0.02454
Zhangjiajie	(a) Scattered	0.02045
Zhangjiakou	(b) Diffused along the urban expansion direction	0.02950
Zhangye	(a) Scattered	0.02674
Zhangzhou	(b) Diffused along the urban expansion direction	0.02629
Changchun	(c) Linear concentrated along arterial roads	0.02136
Changsha	(a) Scattered	0.02177
Changzhi	(a) Scattered	0.02627
Zhaotong	(b) Diffused along the urban expansion direction	0.02302
Zhaoqing	(a) Scattered	0.02348
Zhenjiang	(a) Scattered	0.02602
Zhengzhou	Cities that combine the (b) and (c) characteristics	0.02563
Zhongshan	(a) Scattered	0.02256
Chongqing	(b) Diffused along the urban expansion direction	0.02181
Zhoushan	(a) Scattered	0.01961
Zhoukou	(a) Scattered	0.03926
Zhuhai	(a) Scattered	0.02239
Zhuzhou	(b) Diffused along the urban expansion direction	0.02674
Zhumadian	(b) Diffused along the urban expansion direction	0.03649
Ziyang	(a) Scattered	0.02086
Zibo	(c) Linear concentrated along arterial roads	0.03037
Zigong	(c) Linear concentrated along arterial roads	0.02381
Zunyi	(a) Scattered	0.02367

Supplementary Material

Auditing guidance for physical disorder

Jingjia CHEN, Long CHEN, Yan LI, Wenjia ZHANG, Ying LONG

Physical disorder is a main characteristic in neighborhood environment

As opposed to “Order”, which symbolizes safety, stability and cleanliness, Physical disorder is considered to be the problem of the physical environment of the public space of the neighborhood, referring to the observable or perceived phenomenon or characteristic that indicates the loss of social order, loss of control and spatial deterioration (Cornwell, 2014; Ross & Mirowsky, 1999; Skogan, 1990; Wilson & Kelling, 1982), such as abandoned buildings, street trash, etc.

physical disorder

It is manifested by the deterioration and decline of the urban landscape, usually characterized by vacant buildings, garbage, abandoned vehicles, etc.

social disorder

Refers to people-related, lack of social control and threatening phenomena, such as tyranny in public places, etc.

Data source： Tecent Street View & Baidu Picture

Based on literature review, field survey and manual auditing, an indicator list of physical disorder in Chinese cities is create

1
Architecture

1.1 abandoned building
1.2 building s with damaged facades
1.3 buildings with unkempt facades
1.4 Graffiti/illegal ads
1.5 illegal/temporary buildings

2
Commerce

2.1 stores with poor signboards
2.2 stores with poor facades
2.3 vacant and pending stores

3
Road

3.1 broken roads
3.2 roads stacked with personal belongings
3.3 garbage/litter on street

4
Greening

4.1 messy and unmaintained greening

5
Other infrastructure

5.1 broken infrastructure
5.2 damaged public interface
5.3 construction fence remnant

Example

1.1 abandoned building

Definition:
A building that has been abandoned, unused, or is being demolished

Visual features:
1）There is an obvious "demolition" of the spray paint
2）Unpacked wood slats on doors and windows

** All the images in the rest of this handbook were derived from Tencent Street View*

SPATIAL DISORDER FACTORS AND AUDITING GUIDANCES

Physical disorder		Examples of Street view images	Auditing guidance	Comments
			1）If any of the following visual features appear, the spatial disorder element is considered to "exist"； 2）Regardless of the distance or size of the line of sight in the image, it is counted when it appears.	
1 Architecture	1.1 abandoned building	 	**Definition:** A building that has been abandoned, unused, or is being demolished **Visual features:** 1) There is an obvious "demolition" of the spray paint; 2) Unpacked wood slats on doors and windows.	1) Only construction waste occurs, not included in this item； 2) Buildings under construction are not included in this item.
	1.2 buildings with damaged facades	 	**Definition:** refers to a building with certain damage to the facade; **Visual features:** 1) The degree of damage is high, such as obvious large-area wall loss; 2) The degree of damage is relatively light, such as damage to	1) Buildings under construction are not included in this item.

Physical disorder	Examples of Street view images	Auditing guidance	Comments
		1）If any of the following visual features appear, the spatial disorder element is considered to "exist"； 2）Regardless of the distance or size of the line of sight in the image, it is counted when it appears.	
		facade doors and windows, damage to facade materials, peeling, etc.	
1.3 buildings with unkempt facades	 	**Definition:** refers to a building with obvious stains on the facade; **Visual features:** 1) Facade yellowing, rain stains, rust, etc.; 2) Dust coverage.	1) Old-fashioned buildings that are maintained clean and free of contamination are not included in this item; 2) Contamination and oldness of the bottom shop are only counted in the item "Old pavement".
1.4 graffiti or illegal ads	 	**Definition:** refers to the appearance of unauthorized graffiti or small advertisements on the facade of a building; **Visual features:** 1) Text or pattern graffiti spray paint, emphasizing	1) Graffiti or small advertisements have been removed or cleaned up, showing obvious traces after cleaning, which also

Physical disorder		Examples of Street view images	Auditing guidance	Comments
			1）If any of the following visual features appear, the spatial disorder element is considered to "exist"； 2）Regardless of the distance or size of the line of sight in the image, it is counted when it appears.	
			scribbles, not artistic; 2) small advertisement.	needs to be included in this item.
	1.5 illegal or temporary building	 	**Definition:** refers to illegal structures with public hidden dangers built without permission and without permission; **Visual features:** 1) poor building materials are often used; 2) additional building structures; 3) temporary installations.	1) Mobile box rooms in construction sites and industrial parks are not included in this item.
2 Commerce	2.1 stores with poor signboards	 	**Definition:** Refers to signs of defacement, dilapidation and other signs of shops along the street that have not been cleaned and maintained; **Visual features:** 1) signboard defaced; 2) signboard damaged.	1) There are many signboards and various colors, which are not included in this item.

Physical disorder	Examples of Street view images	Auditing guidance	Comments
		1）If any of the following visual features appear, the spatial disorder element is considered to "exist"； 2）Regardless of the distance or size of the line of sight in the image, it is counted when it appears.	
2.2 stores with poor facades		**Definition:** Refers to the signs of contamination and dilapidation of the doors, windows, glass, etc. of shops along the street due to lack of timely maintenance; **Visual features:** 1) Extensive stains on doors or windows or glass, etc.	
2.3 vacant and pending stores		**Definition:** means a business that is closed, unoccupied, vacant or for sale; **Visual features:** 1) The characters "for sale" and "for sale" appear on the facade; 2) there are obvious door locks and seals in the store; 3) the store has rolling shutters that are down and closed.	

Physical disorder		Examples of Street view images	Auditing guidance	Comments
			1）If any of the following visual features appear, the spatial disorder element is considered to "exist"; 2）Regardless of the distance or size of the line of sight in the image, it is counted when it appears.	
3 Road	3.1 broken roads	 	**Definition:** It is manifested as damage to the hardened pavement or curb, which affects the passage; **Visual features:** 1) Cracks on the road; 2) Potholes on the road; 3) Damaged curbs.	1) Water stains on the road surface are not included in this item.
	3.2 roads stacked with personal belongings	 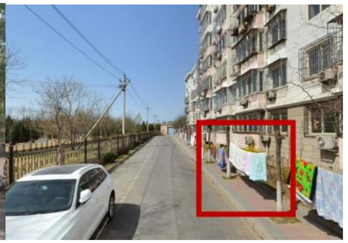	**Definition:** Refers to the accumulation of private items and encroaching on public space, affecting the use and passage; **Visual features:** 1) Merchants and shops are placed outside; 2) Sundries are stacked.	1) Illegal parking or cars occupying the sidewalk are not included in this item.

Physical disorder		Examples of Street view images	Auditing guidance	Comments
			1）If any of the following visual features appear, the spatial disorder element is considered to "exist"； 2）Regardless of the distance or size of the line of sight in the image, it is counted when it appears.	
	3.3 garbage or litter on street		**Definition:** refers to the accumulation or distribution of garbage that obviously affects the cleanliness of the street and is not collected and transported in time; **Visual features:** 1) Garbage accumulation; 2) Garbage that obviously affects the cleanliness of the ground is scattered and discarded.	1) Domestic waste, construction waste, etc. are included in this item.
4 Greening	4.1 messy and unmaintained greening		**Definition:** Refers to the cluttered phenomenon caused by the lack of regular maintenance and sanitation repair of municipal greening in urban areas; **Visual features:** 1) Large weeds that destroy the integrity of the landscape; 2) Shrubs that have not been pruned for a long time and make the shape too	1) The countryside and wheat fields in non-urban areas are not included in this item.

Physical disorder		**Examples of Street view images**	**Auditing guidance** 1）If any of the following visual features appear, the spatial disorder element is considered to "exist"； 2）Regardless of the distance or size of the line of sight in the image, it is counted when it appears.	**Comments**
			irregular; 3) Vegetation that is yellow and dry without regular watering and replacement, etc.	
5 Other infrastructure	5.1 broken infrastructure		**Definition:** Refers to signs of damage to infrastructure such as wires, street lights, and distribution boxes that have not been maintained; **Visual features:** 1) The utility pole is crooked; 2) A large number of ungrounded wires are scattered; 3) The electrical box is damaged.	

Physical disorder	Examples of Street view images	Auditing guidance	Comments
		1）If any of the following visual features appear, the spatial disorder element is considered to "exist"； 2）Regardless of the distance or size of the line of sight in the image, it is counted when it appears.	
5.2 damaged public interface		**Definition:** Refers to signs of damage to walls or fences in public spaces; **Visual features:** 1) Broken fence; 2) Broken fence.	
5.3 construction fence remnant		**Definition:** Refers to construction enclosures that are obviously dilapidated or defaced and affect the cleanliness of the street; **Visual features:** 1) The construction enclosure is dilapidated; 2) The construction enclosure is damaged in a large area.	

Some examples

Whether "abandoned building" is appeared in these images?

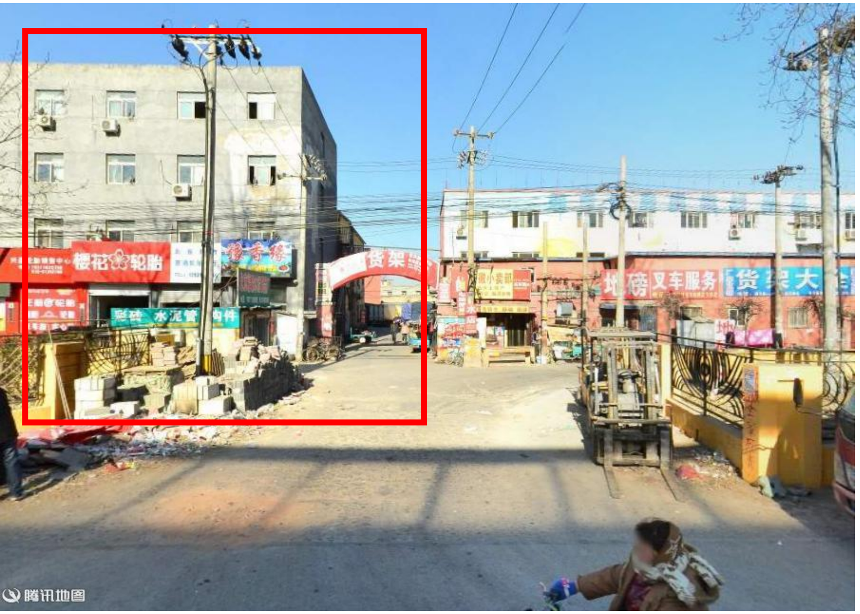

NO
Only opened windows

YES
Typical abandoned building

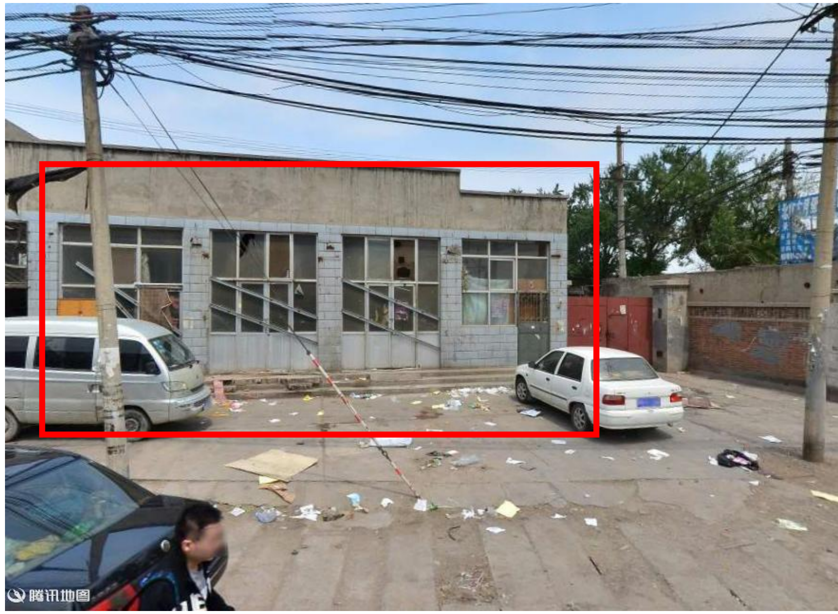

YES
With wood slats

1 Architecture

ITEMS

Whether “buildings with damaged facades” is appeared in these images?

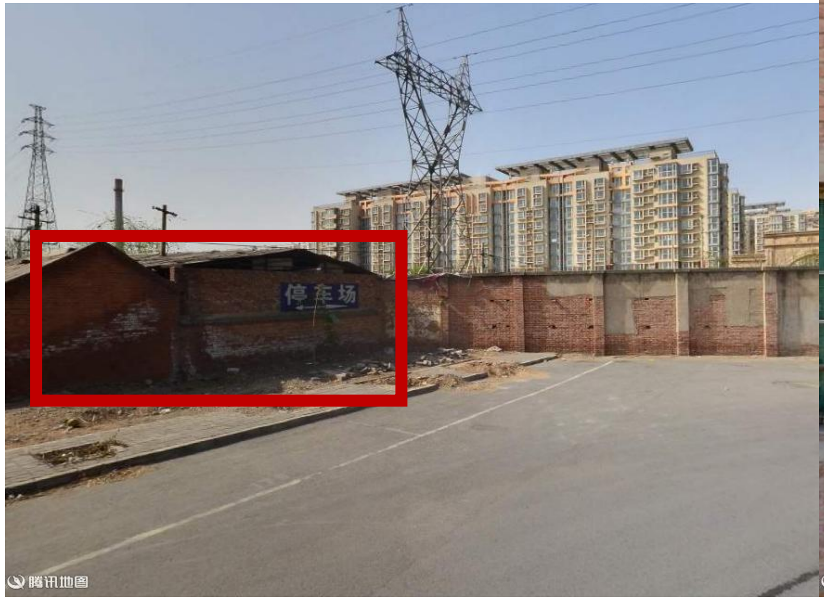

YES
Typical damaged facades

YES
Even is has been repaired

NO
Stains refers to unkempt facades

Whether "buildings with unkempt facades" is appeared in these images?"

NO
Old age

NO
Stores with poor facades

YES
Smudge marks appear

Whether “graffiti/illegal ads” is appeared in these images?

NO
Has been removed

YES
Although removed, but still messy

YES
Typical illegal ads

Whether “illegal/temporary building” is appeared in these images?

YES
Typical illegal building

YES
Typical temporary building

3 Road

Whether “broken roads” is appeared in these images?

YES
Typical broken roads

YES
Including sidewalks

YES
Including curbs

Whether "garbage/litter on street" is appeared in these images? "

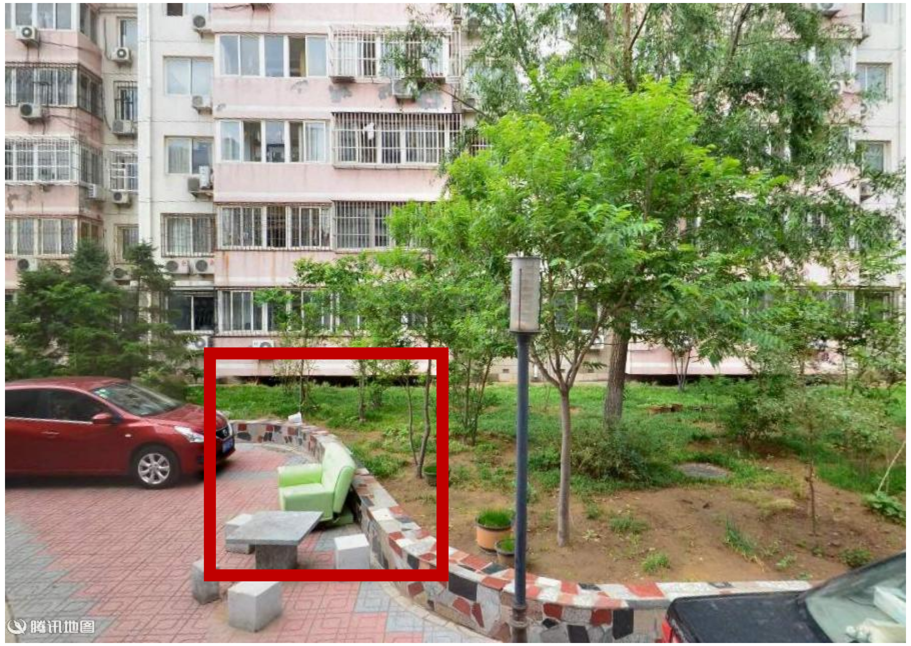

YES
Typical litter on street

NO
Functioning street furniture

Whether "messy and unmaintained greening" is appeared in these images?

YES
Bare soil in greening

YES
Typical messy greening

NO
Seasonal dryness

Whether "construction fence remnant" is appeared in these images?

NO
Only when the fence is dirty

YES
Rust has appeared

American Association of Geographers

P.O. Box 73158
Washington, DC 20056
Voice 202-234-1450
Fax 202-234-2744
gaia@aag.org
http://www.aag.org

AAG Councilors

President
Marilyn Raphael
University of California Los Angeles

Vice President
Rebecca Lave
Indiana University Bloomington

Past President
Emily T. Yeh
University of Colorado at Boulder

Secretary
Joseph Oppong
University of North Texas

Treasurer
Marcia England
Miami University

Heike Alberts
University of Wisconsin Oshkosh

Pablo Bose
University of Vermont

Meghan Cope
University of Vermont

Dydia DeLyser
California State University, Fullerton

Tracy Edwards
Frostburg State University

Debarchana Ghosh
University of Connecticut

Colleen Myles
Texas State University

Shannon O'Lear
University of Kansas

Diana Ojeda
Universidad de los Andes

Steven M. Schnell
Kutztown University of Pennsylvania

Steven Silvern
Salem State University

Patricia Solís
Arizona State University

Selima Sultana
University of North Carolina Greensboro

Edna Wangui
Ohio University

Executive Director
Gary Langham

Dr. Ying Long
Associate Professor
Department of Urban Planning
Tsinghua University
Beijing, China, 100084

October 20, 2022

Dear Dr. Ying Long,

This letter serves as a Certificate of Recognition of your role as corresponding author for the following article, which was accepted by Editor Ling Bian on July 8, 2022 for publication in the *Annals of the American Association of Geographers*: Measuring Physical Disorder in Urban Street Spaces: A Large-Scale Analysis Using Street View Images and Deep Learning, by Jingjia Chen, Long Chen, Yan Li, Wenjia Zhang & Ying Long. Your article is published at Taylor & Francis Online: https://doi.org/10.1080/24694452.2022.2114417.

The *Annals of the American Association of Geographers* is a scholarly publication of the American Association of Geographers.

Thank you for your contribution to the *Annals of the American Association of Geographers*.

Best wishes,

Jennifer Cassidento
Publications Director and Journals Managing Editor
American Association of Geographers
1710 Sixteenth Street NW
Washington, DC 20009-3198
E-mail: jcassidento@aag.org
Website: www.aag.org